AIP Journal of Applied Physics

Optical characterization of individual GaAs quantum dots grown with height control technique

F. Sarti, G. Muñoz Matutano, S. Bietti, A. Vinattieri, S. Sanguinetti et al.

Citation: J. Appl. Phys. **114**, 124301 (2013); doi: 10.1063/1.4821901
View online: http://dx.doi.org/10.1063/1.4821901
View Table of Contents: http://jap.aip.org/resource/1/JAPIAU/v114/i12
Published by the AIP Publishing LLC.

Additional information on J. Appl. Phys.

Journal Homepage: http://jap.aip.org/
Journal Information: http://jap.aip.org/about/about_the_journal
Top downloads: http://jap.aip.org/features/most_downloaded
Information for Authors: http://jap.aip.org/authors

ADVERTISEMENT

physics today
Read author interviews in Bookends

Downloaded 26 Sep 2013 to 158.42.44.159. This article is copyrighted as indicated in the abstract. Reuse of AIP content is subject to the terms at: http://jap.aip.org/about/rights_and_permissions

JOURNAL OF APPLIED PHYSICS **114**, 124301 (2013)

Optical characterization of individual GaAs quantum dots grown with height control technique

F. Sarti,[1] G. Muñoz Matutano,[1,a)] S. Bietti,[2] A. Vinattieri,[1] S. Sanguinetti,[2] and M. Gurioli[1]
[1]*Dipartimento di Fisica e Astronomia, LENS and CNISM, Università di Firenze, Via Sansone 1, I-50019 Firenze, Italy*
[2]*Dipartimento di Scienza dei Materiali and L-NESS, Università di Milano Bicocca, Via Cozzi 53, I-20125 Milano, Italy*

(Received 11 July 2013; accepted 5 September 2013; published online 23 September 2013)

We show that the epitaxial growth of height-controlled GaAs quantum dots, leading to the reduction of the inhomogeneous emission bandwidth, produces individual nanostructures of peculiar morphology. Besides the height controlled quantum dots, we observe nanodisks formation. Exploiting time resolved and spatially resolved photoluminescence we establish the decoupling between quantum dots and nanodisks and demonstrate the high optical properties of the individual quantum dots, despite the processing steps needed for height control. © *2013 AIP Publishing LLC*. [http://dx.doi.org/10.1063/1.4821901]

Nanotechnologies are of great interest for classical and quantum optoelectronics and photonic applications.[1] Semiconductor quantum dots (QDs) are nowadays the main building blocks for innovative and high performances optoelectronic devices, such as lasers, light emitting diodes, visual displays, and photovoltaic solar cells.[1] Solid state quantum light sources, such as single photon or entangled photon pair emitters, can be also achieved by exploiting the exciton and biexciton cascade in individual QDs.[2] In all these applications the control of the size and shape of the nanostructures is of great importance for the tailoring of the device optical properties. In particular it has been recently pointed out that the near infrared and red emission is a central issue for hybrid quantum network based on solid state qu-bits and cold Rb atoms: such spectral region can be easily targeted by GaAs/AlGaAs QDs grown by droplet epitaxy (DE).[3–5]

A further advantage of GaAs/AlGaAs QDs is the absence of strain in the QD layers which avoids changes in the QD morphology and composition after the capping procedure.[6] The strain-free GaAs/AlGaAs nanostructures can be tailored in many different shapes, from QDs to multiple rings, by small variations of the growth parameters.[7–10] This is made possible owing to the DE growth method, which allows for the fine control of the kinetics of the transformation from nanoscale metal droplets to III–V nanocrystals.[5] However, typical DE-QD emission spectra show quite large, inhomogeneously broadened, bands in the 60–100 meV range, which are the outcome of the initial size dispersion of the droplet, from which the QDs are formed, and of the complex crystallization dynamics.[11,12] Recently a morphological control of the QD heights has been proposed by using a thin AlGaAs capping layer and *in situ* annealing,[13] with the flattening of the top of the QDs, leading to the reduction of the inhomogeneous emission bandwidth from a large ensemble of high density QDs with superior uniformity; this property has been exploited for building laser diodes.

Despite the fundamental and applicative relevance of the technique for the formation of height-controlled QDs, very little is known either on the optical quality of the *in situ* annealed QDs or on the role of the GaAs removed by annealing. In this contribution we exploit time resolved and spatially resolved micro photoluminescence to establish the optical properties of the individual QDs after the height control process and to address the effects of GaAs diffusion from the top of the QDs as a consequence of the cut of the QD top. We will show that the optical quality of the QDs is quite high and that the cut of the QD top results in the formation of families of nanodisks (NDs) with different heights. The study of the recombination kinetics and spatial localization of the QDs and NDs emission demonstrates that the different nanostructures are not electronically coupled.

Samples were grown on semi-insulating GaAs(001) substrates by molecular beam epitaxy and characterized *in situ* by reflection high energy electron diffraction (RHEED) and *ex situ* by atomic force microscopy (AFM). AFM measurements were performed in tapping mode using ultra-sharp tips with a 2 nm radius. The growth of high-quality morphology controlled GaAs QDs by DE consists of several steps: (i) deposition of metallic Ga droplets; (ii) crystallization of the Ga droplets into GaAs QDs via of the As flux supply and, (iii) deposition of a thin AlGaAs capping layer followed by a high-temperature annealing. The effectiveness of each of these processes is discussed later. After the growth of 500 nm GaAs buffer layer and 150 nm $Al_{0.3}Ga_{0.7}As$ layer at 580 °C, the substrate temperature was lowered to 350 °C, the As flux was closed, and the As pressure inside the chamber decreased below 2×10^{-9} Torr. $c(4 \times 4)$ reconstruction, in $c(4 \times 4)\alpha$ phase,[14] was detected in the RHEED pattern. 1.1 monolayers (MLs) of Ga were then deposited to form Ga droplets at 0.07 ML s^{-1}. The formation of droplets on the surface was checked by AFM. The Ga droplet density was 5×10^8 cm^{-2}. The Ga droplets were crystallized into GaAs islands by means of an As_4 flux of 5×10^{-5} Torr at the

[a)]Present address: Instituto de Ciencia de los Materiales, Universidad de Valencia, P.O. Box 22085, 46071 Valencia, Spain.

 © 2013 AIP Publishing LLC

Downloaded 26 Sep 2013 to 158.42.44.159. This article is copyrighted as indicated in the abstract. Reuse of AIP content is subject to the terms at: http://jap.aip.org/about/rights_and_permissions

substrate temperature of 150 °C. After crystallization, the average dot radius was 25 nm and the height 10 nm. Subsequently, the QDs were annealed at 400 °C for 10 min under an As_4 flux of 6×10^{-6} Torr without capping. This step, while strongly improving the QD optical quality,[15] only slightly influences the dot shape, reducing the dot height and increasing the dot anisotropy.[16] The QDs were then covered with 4 nm $Al_{0.3}Ga_{0.7}As$ layer grown by migration enhanced epitaxy.[17] A second annealing step was performed at 620 °C and 6×10^{-6} Torr of As for 20 min to induce a selective mass redistribution at the top of the QDs.[13] Typical AFM maps of the QDs partially covered with 4 nm of AlGaAs is shown in Figure 1 before (Figure 1(a)) and after (Figure 1(b)) 10 min of annealing at 620 °C. The surface of the sample, after the 620 °C annealing step, is flat (0.7 nm RMS), with no visible hills or holes marking the position of the partially covered QDs before annealing. Finally, the QDs were capped with a 100 nm $Al_{0.3}Ga_{0.7}As$ grown at 580 °C and 10 nm GaAs. Post growth *ex situ* annealing at 800 °C for 4 min is used to improve the optical quality of the QDs.

Photoluminescence (PL) measurements were performed by keeping the sample placed in a cold-finger cryostat to control the temperature. Different excitation conditions were used: continuous wave measurements were performed by a frequency-doubled Nd-yttrium aluminium garnet laser $\lambda_{exc} = 532$ nm, and time resolved experiments were performed exciting the sample with the second harmonic $\lambda_{exc} = 400$ nm of a mode-locked Ti:sapphire laser pumped by a continuous wave Ar^+ laser providing 1.2-ps pulses at a repetition rate of 82 MHz. In case of time resolved PL, the signal was dispersed through a 30-cm flat-field monochromator and detected by a streak camera apparatus with a 3-ps time resolution. In the microPL setup, the laser spot size on the sample was of the order of 3 μm. In detection we used a confocal setup for μ-PL measurements (with a single mode fiber in detection acting as a pinhole, main objective 100×, NA = 0.7) leading to a lateral resolution of about 1.0 μm. The collected PL was dispersed by a monochromator and detected by a silicon charge coupled device camera.

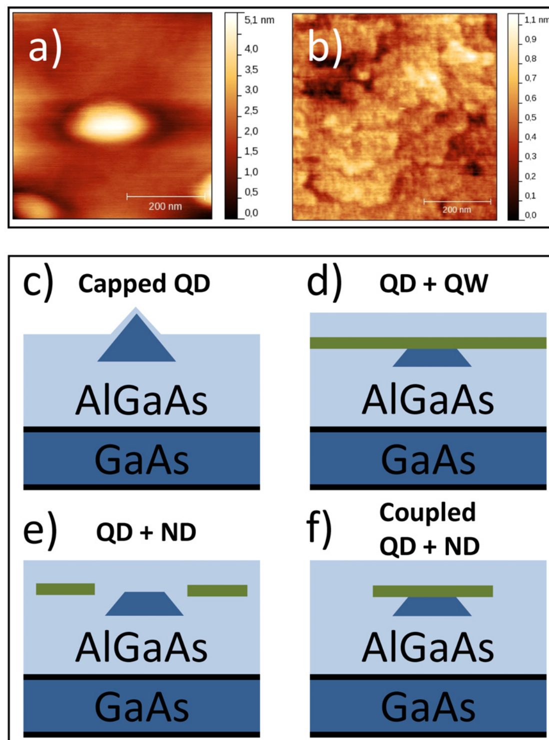

FIG. 1. (a) and (b) AFM images of QDs partially covered with 4 nm of AlGaAs. (a) Surface before annealing, (b) surface after 10 min of annealing at 620 °C. (c)–(f) Schematic of the QDs height control process. (c) Picture of a QDs which is cover by the 4 nm height AlGaAs layer. (d)–(f) Different possible pictures of the distribution of the GaAs excess: (d) formation of a thin QW, (e) formation of disconnected nanodisks, (f) formation of a mushroom like QDs.

Let us start with a schematic of the different possible QD morphology during the *in situ* annealing, as shown in Figures 1(c)–1(f). After the droplet formation and the QD crystallization we end up with a large variety of QD heights, related to the Ga size dispersion (around 30% in the present sample). The capping with 4 nm thick layer of AlGaAs, while entirely covering the surface, is expected to be thinner on the convex QD top, due to capillarity effects.[18] This divides the dot volume in two parts: (1) the bottom part, completely buried within the AlGaAs layer covering the surface and (2) the top part, covered by a very thin AlGaAs layer, protruding over the surface (Figs. 1(a) and 1(c)). During the *in situ* annealing the protruding top of the QDs tends to diffuse on the AlGaAs layers, leading either to a thin quantum well (QW) on the top of the decapped QDs (Fig. 1(d)) or to a series of nanostructures not connected to the QDs (Fig. 1(e)) or, finally, to a ND on the top of the QDs which may lead to an electronically coupled mushroom like nanostructure (Fig. 1(f)). The expected composition of the diffusion related structures is GaAlAs with an extremely low Al content. The aim of this paper is twofold, on one side we would like to assess the optical quality of the individual QDs after the cut of their top, on the other side we intend to understand which type of nanostructure is fabricated with the height control process.

Figure 2(a) shows typical macroPL spectra for different temperatures in the range 10 K–200 K. Referring to the spectrum at T = 10 K, we observe the QDs PL band at 1.72 eV with a full width at half maximum of 30 meV. In fact the PL-FWHM value is quite small if compared with DE QDs growth without the height control process, where the FWHM can be as large as 100 meV. Note also that the QD emission at 1.72 eV means a confinement energy of 200 meV in the GaAs QDs. Due to the quadratic dependence of the confinement energy on the QD size, we can estimate a variance of the QD size of the order of 7%, denoting the superior uniformity of the QD size distribution. The emission at 1.93 eV is clearly associated with the excitonic recombination in the AlGaAs layer. Finally the multistructured PL spectrum between 1.8 and 1.9 eV is due to the additional nanostructures generated by the diffusion of the excess GaAs after the cut of the QD height during the *in situ* annealing. The lineshape of this PL spectrum is typical of nanostructures (either QWs or NDs) with different number of GaAs MLs in height as, for example, observed in QWs after growth interruption at the interfaces. From effective mass model we attribute the peak at 1.82 eV to 5MLs, the peak at 1.85 eV to 4 MLs, and the peak at 1.88 eV to 3 MLs.

Downloaded 26 Sep 2013 to 158.42.44.159. This article is copyrighted as indicated in the abstract. Reuse of AIP content is subject to the terms at: http://jap.aip.org/about/rights_and_permissions

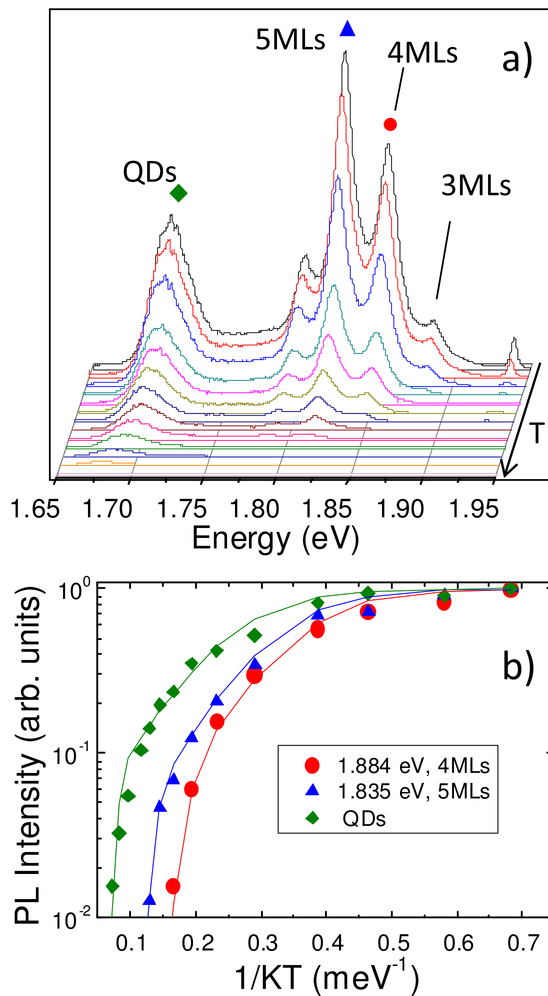

FIG. 2. (a) MacroPL spectra at different temperatures. (b) Arrhenius plots for the QDs (green diamonds), the 5 MLs (blue triangles), and the 4 MLs (red circles).

The spectra change when increasing the temperature; besides, the gap shrinking Figure 2(a) shows that the PL quenching of the different spectral component turns out to be activated at lower temperatures—the higher is the emission energy. The Arrenhius plots in Figure 2(b) refer to the QDs (green diamonds) and to the two most intense additional spectral contributions corresponding to 5 MLs (blue triangles) and 4 MLs (red circles). The fits of the data with two thermally activated nonradiative channels give a first activation energy of 30 meV common to all the spectral contributions, likely due to the quenching of the carrier capture efficiency in the nanostructures. The second activation energy is different in the three emissions, and it is in quite good agreement with a carrier escape towards the AlGaAs barrier states. These data point out the lack of thermalization between the states of the different nanostructures.

Additional information comes out from the time resolved PL analysis; typical decays curves are reported in Figure 3 for the QDs, the additional nanostructures and the AlGaAs layers. The most important feature is that the PL rise time of the QDs and the additional nanostructures is similar and in the range of 30 ps while the rise time of the AlGaAs recombination is much faster and almost resolution

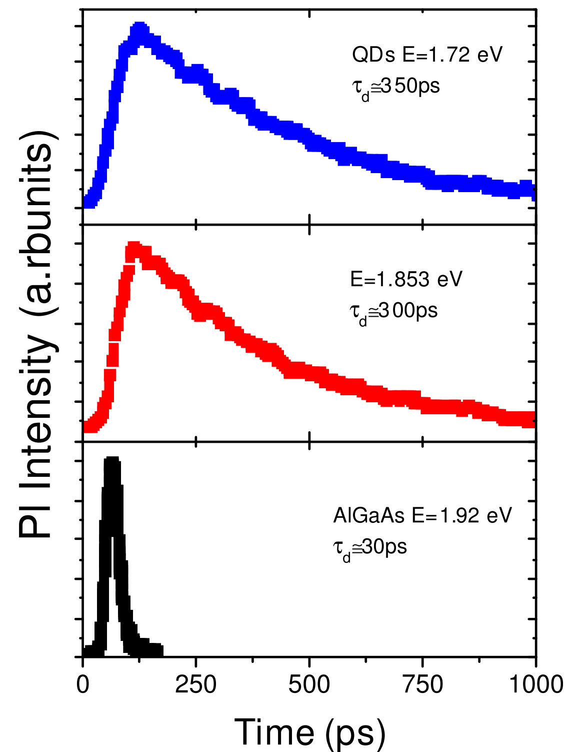

FIG. 3. Decay spectra of the different emission lines. The values of the decay times as obtained from exponential fits are also given.

limited (below 10 ps). In addition the decay time of the AlGaAs recombination is also of the order of 30 ps, denoting that the carrier lifetime in the AlGaAs layer is due to the carrier capture by the QDs and additional nanostructures. The decay time of the QD-PL is of the order of 350 ps while the emission from the additional nanostructures is a bit faster with a recombination time of the order of 300 ps. Clearly the picture of a recombination cascade from the higher energy states of the additional nanostructures towards the lower energy states of the QDs is washed out by the observed recombination kinetics. This result, in addition with the lack of thermalization, clearly excludes the hypothesis of a QW (Fig. 1(d)) created with the excess GaAs. We therefore expect that the additional nanostructures are likely NDs with

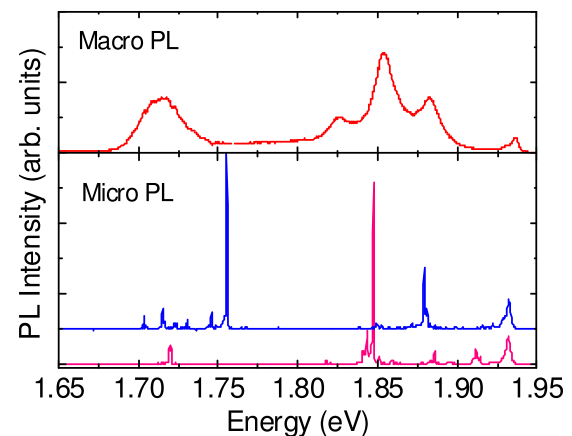

FIG. 4. Comparison between the macroPL (top line) and two microPL (bottom lines) spectra. In microPL we usually resolved few individuals QDs and NDs.

Downloaded 26 Sep 2013 to 158.42.44.159. This article is copyrighted as indicated in the abstract. Reuse of AIP content is subject to the terms at: http://jap.aip.org/about/rights_and_permissions

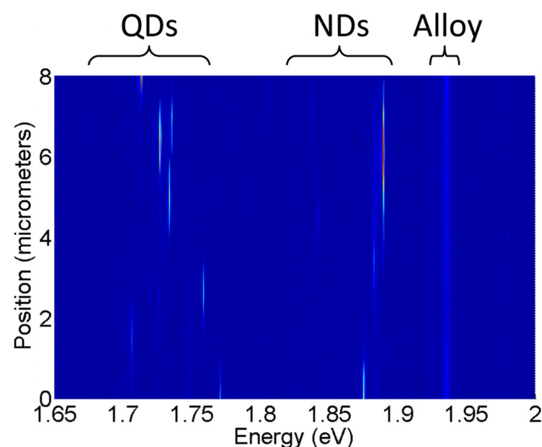

FIG. 5. Spatially resolved map of the PL emissions.

few monolayer of GaAs in height. In addition our data also tend to exclude any electronic coupling between the QDs and the NDs.

The measured lifetime and the high brightness of the QD PL denote the lack of relevant non radiative channels and therefore assess an overall good optical quality of the sample. However in order to get detailed information on the optical properties of the individual nanostructures we performed a series of microPL measurements. The comparison between the macroPL and two different microPL spectra is reported in Figure 4. Within the spatial resolution of our confocal microscope we can resolve the emission from few individual nanostructures, both in the QDs and in the NDs region and in both cases, sharp and intense emission lines are resolved. The spectral width of the QD lines are, in a statistics of 15 different cases, below our resolution limit which is of the order of 250 μeV. This denotes that the process involved in the height control of the quantum dots is not detrimental for the quality of the DE QDs in terms of impurities contamination and consequent large spectral diffusion. It is worth remembering that one of the possible disadvantages of the DE growth is that low temperature growth tends to produce a quite large spectral diffusion in the individual QD emission.

A typical spatial map of the microPL spectra is reported in Figure 5 where the different spectral regions are marked in the top of the map. Interestingly the emission from the AlGaAs excitonic recombination is completely delocalized over the whole spatial scanning. On the contrary both the NDs and the QD emissions are spatially localized with a spatial extension of the order of 1 μm which stems from our experimental resolution. The most striking aspect of these data is the fact that the QD and ND emission are spatially separated. This means that the real picture for the morphological configuration of the sample after the height control process is given by Fig. 1(e). The absence of overlap between the QDs and NDs completely explain the lack of thermalization and population transfer during the recombination kinetics.

In conclusion we have performed a complete characterization of the optical properties of QD samples grown with height control techniques. We demonstrate that the diffusion of the GaAs excess in large QDs during the *in situ* annealing leads to the formation of NDs in the layer above the QDs. These NDs are spatially separated by the QDs and are not involved in the QD carrier capture or in the carrier thermalization and recombination kinetics. Finally we have assessed that the protocol for the QD height control is not detrimental for the QD optical quality and therefore can be used to improve the QD homogeneity not only in the design of standard optoelectronic devices such as laser but also in application to quantum photonics.

[1]M. Grundmann, *The Physics of Semiconductors* (Springer, Berlin, 2006).
[2]A. Shields, Nat. Photonics **1**, 215 (2007).
[3]N. Koguchi and K. Ishige, "New selective molecular beam epitaxial growth method for direct formation of GaAs quantum dots," J. Vac. Sci. Technol. B **11**(3), 787 (1993).
[4]K. Watanabe, N. Koguchi, and Y. Gotoh, "Fabrication of GaAs quantum dots by modified droplet epitaxy," Jpn. J. Appl. Phys. **39**(2), L79 (2000).
[5]S. Sanguinetti and N. Koguchi, "Droplet epitaxy of nanostructures," in *Molecular Beam Epitaxy from Research to Mass Production*, edited by M. Henini (Elsevier Ltd., 2013), p. 95.
[6]J. G. Keizer, J. Bocquel, P. M. Koenraad, T. Mano, T. Noda, and K. Sakoda, "Atomic scale analysis of self assembled GaAs/AlGaAs quantum dots grown by droplet epitaxy," Appl. Phys. Lett. **96**(6), 062101 (2010).
[7]T. Mano, T. Kuroda, S. Sanguinetti, T. Ochiai, T. Tateno, T. Noda, M. Kawabe, K. Sakoda, G. Kido, N. Koguchi, and J. S. Kim, "Self-assembly of concentric quantum double rings," Nano Lett. **5**(3), 425 (2005).
[8]J. H. Lee, Z. M. Wang, Z. Y. Abuwaar, N. W. Strom, and G. J. Salamo, "Evolution between self-assembled single and double ring-like nanostructures," Nanotechnology **17**(15), 3973–3976 (2006).
[9]C. Somaschini, S. Bietti, N. Koguchi, and S. Sanguinetti, "Coupled quantum dot–ring structures by droplet epitaxy," Nanotechnology **22**(18), 185602 (2011).
[10]C. Somaschini, S. Bietti, N. Koguchi, and S. Sanguinetti, "Fabrication of multiple concentric nanoring structures," Nano Lett. **9**(10), 3419 (2009).
[11]K. Reyes, P. Smereka, D. Nothern, J. M. Millunchick, S. Bietti, C. Somaschini, S. Sanguinetti, and C. Frigeri, "Unified model of droplet epitaxy for compound semiconductor nanostructures: Experiments and theory," Phys. Rev. B **87**(16), 165406 (2013).
[12]S. Bietti, C. Somaschini, and S. Sanguinetti, "Crystallization kinetics of Ga metallic nano-droplets under As flux," Nanotechnology **24**, 205603 (2013).
[13]M. Jo, T. Mano, and K. Sakoda, "Morphological control of GaAs quantum dots grown by droplet epitaxy using a thin AlGaAs capping layer," J. Appl. Phys. **108**(8), 083505 (2010).
[14]A. Ohtake, "Surface reconstructions on GaAs(001)," Surf. Sci. Rep. **63**(7), 295 (2008).
[15]T. Mano, M. Abbarchi, T. Kuroda, C. A. Mastrandrea, A. Vinattieri, S. Sanguinetti, K. Sakoda, and M. Gurioli, "Ultra-narrow emission from single GaAs self-assembled quantum dots grown by droplet epitaxy," Nanotechnology **20**(39), 395601 (2009).
[16]S. Adorno, S. Bietti, and S. Sanguinetti, "Annealing induced anisotropy in GaAs/AlGaAs quantum dots grown by droplet epitaxy," J. Cryst. Growth **378**, 515 (2013).
[17]Y. Horikoshi, M. Kawashima, and H. Yamaguchi, "Migration-enhanced epitaxy of GaAs and AlGaAs," Jpn. J. Appl. Phys. **27**(2), 169 (1988).
[18]G. Biasiol, A. Gustafsson, K. Leifer, and E. Kapon, "Mechanisms of self-ordering in nonplanar epitaxy of semiconductor nanostructures," Phys. Rev. B **205**, 306 (2002).

Downloaded 26 Sep 2013 to 158.42.44.159. This article is copyrighted as indicated in the abstract. Reuse of AIP content is subject to the terms at: http://jap.aip.org/about/rights_and_permissions